Nanoscale

PAPER

Upconversion fluorescent strip sensor for rapid determination of *Vibrio anguillarum*

Cite this: DOI: 10.1039/c3nr06549a

Peng Zhao,[a] Yuanyuan Wu,[b] Yihua Zhu,*[a] Xiaoling Yang,[a] Xin Jiang, Jingfan Xiao,[b] Yuanxing Zhang[b] and Chunzhong Li*[a]

Received 10th December 2013
Accepted 7th January 2014

DOI: 10.1039/c3nr06549a

www.rsc.org/nanoscale

Here, we report a simple and ultrasensitive upconversion fluorescent strip sensor based on $NaYF_4$:Yb,Er nanoparticles (NPs) and the lateral flow immunochromatographic assay (LFIA). Carboxyl-modified β-$NaYF_4$:Yb,Er NPs were successfully synthesized by a facile one-pot solvothermal approach, upon further coupling with monoclonal antibody, the resultant UCNPs-antibody conjugates probes were used in LFIA and served as signal vehicles for the fluorescent reporters. *V. anguillarum* was used as a model analyte to demonstrate the use of this strip sensor. The limit of the detection for the fluorescent strip was determined as 10^2 CFU mL^{-1}, which is 100 times lower than those displayed by enzyme-linked immunosorbent assays, while the time needed for the detection was only 15 min. Furthermore, no cross-reaction with other eight pathogens was found, indicating the good specificity of the strip. This developed LFIA would offer the potential as a useful tool for the quantification of pathogens analysis in the future.

1. Introduction

Vibriosis is a systemic infection, primarily of marine and estuarine fish, which produces either skin ulcers or a septicemia characterized by erythema, hemorrhages, and anemia, causing significant mortalities especially in summer when the temperature of the water is above 15 °C.[1] The disease can spread rapidly when fish is confined in heavily stocked, commercial systems and morbidity may reach 100% in affected facilities. This disease is severely damaging the aquaculture industry and exacerbates the shortage of fresh fish and shellfish. The most commonly encountered fish pathogenic Vibrio species is *V. anguillarum*, which is a Gram-negative marine bacterium and the main causative agent of vibriosis.[2] It is a native microflora of the aquatic environment and proportionally increases during the summer season. Consequently, fish may be continually threatened by this opportunistic pathogen which may be able to cause disease under certain predisposing conditions. Because of the devastating effects of this bacterial pathogen, early detection is necessary to avoid mass mortality in cultured fishes. A variety of antibody-based and molecular tests have been developed to detect main bacterial and viral pathogens, such as fluorescent antibody technique, enzyme-linked immunosorbent assay (ELISA), polymerase chain reaction (PCR) and *in situ* hybridization.[3,4] However, these methods have drawbacks. For example, conventional PCR is technically demanding, time consuming and also needs optimization of temperature conditions to perform denaturation, annealing and elongation in a thermocycler. Phenotypic and biochemical methods are primitive and time consuming.[5] Therefore, a more suitable technique is necessary, which can overcome most of the drawbacks that have been mentioned.

Fast, simple and easy-to-operate detection methods are still urgently needed not only in aquaculture industry but also in many fields.[6,7] Hence, many studies have investigated rapid detection methods that are designed to meet the increasing demands. These techniques include the colorimetric method based on the metallic nanoparticles,[8–11] the electrochemical based rapid detection methods[12,13] and also microfluidic chip based methods.[14,15] Of these methods, the gold labeled strips have achieved great success and have been commercialized.[16–18] Immunochromatographic assay, also called lateral flow immunochromatographic assay (LFIA), with benefits of rapid, low-cost, easy-to-use and sensitive detection of various analytes, has been developed for many years and received much attention.[19,20] LFIA is used for the qualitative or semi-quantitative detection of many analytes including antigens, antibodies, and even the products of nucleic acid amplification tests.[21] However, their applications are limited due to the low signal intensity and poor quantitative discrimination of the color-formation reaction based on the label accumulation. So the search for the increased detection sensitivity and the possibility of quantitative detection using simple inexpensive assays is an ongoing challenge.

[a]*Key Laboratory for Ultrafine Materials of Ministry of Education, School of Materials Science and Engineering, East China University of Science and Technology, 130 Meilong Road, Shanghai 200237, China. E-mail: yhzhu@ecust.edu.cn; czli@ecust.edu.cn; Fax: +86 21 6425 0624; Tel: +86 21 6425 2022*

[b]*State Key Laboratory of Bioreactor Engineering, East China University of Science and Technology, 130 Meilong Road, Shanghai 200237, P.R. China*

Here, we introduce the use of upconversion (UC) fluorescent materials as reporters in lateral flow assays. Lanthanide-based upconversion fluorescent materials, which can convert near-infrared (NIR) light to visible light by emitting higher-energy photons after absorbing lower-energy photons, have attracted a tremendous amount of attention.[22–25] The UC fluorescence utilizes NIR excitation rather than ultraviolet (UV) excitation, which can significantly minimize background autofluorescence and photodamage, increase the penetration length in biological tissues, and improve the signal-to-noise ratio and sensitivity in biological detection.[26–28] And in recent years, UC reporters are reported at least 100-fold more sensitive than assays using conventional reporter systems such as colloidal gold or colored latex beads.[29] Among all the UC materials, due to low phonon energy of lattices, hexagonal phase sodium yttrium fluoride (β-$NaYF_4$) crystals have been reported to be one of the most efficient UC host materials and have been widely studied, especially for the systems doped with Yb,Er and Yb,Tm.

In this report, we present, for the first time, on the development of an optical based biosensor which employs UCNPs-labeled monoclonal antibody probe as a reporter for the detection of *V. anguillarum*. Carboxyl-modified β-$NaYF_4$:Yb,Er NPs were prepared with desirable UC fluorescence properties. Due to the advantages derived from UCNPs and LFIA, a rapid, sensitive, specificity strategy has been developed for *V. anguillarum* analysis.

2. Experimental section

2.1 Materials

$RE(NO)_3$ (99.9%) (RE = Y^{3+}, Yb^{3+}, Er^{3+}) and poly(acrylic acid, sodium salt) (PAAs) were obtained from Alfa Aesar Co. Ltd. *N*-Hydroxy-succinimide (NHS) and 1-ethyl-3-(3-dimethylaminopropyl)carbodiimide hydrochloride (EDC) were purchased from J&K Chemical Ltd. All other chemicals were purchased from the Shanghai Chemical Reagent Co. All chemicals were used as received.

The UPNPs-LFIA biosensor was designed and produced *via* collaboration between our laboratory and State Key Laboratory of Bioreactor Engineering, East China University of Science and Technology. The LFIA strips, antigen *V. anguillarum* MVM425 and monoclonal antibody 5G4-G4, 5G4-B8 used in this study were provided by Prof. Yuanxing Zhang from the State Key Laboratory of Bioreactor Engineering. Pathogens of *V. alginolyticus*, *V. parahaemolyticus*, *V. harveyi*, *V. vulnificus*, *Edwardsiella tarda* EIB202, *Streptococcus iniae*, *Escherichia coli* CC118 and *Staphylococcus aureus* were also provided by Prof. Yuanxing Zhang from the State Key Laboratory of Bioreactor Engineering.

2.2 Synthesis of carboxyl-modified β-$NaYF_4$:Yb,Er UCNPs

Typically, 1.2 mmol of $RE(NO_3)_3$ (Y^{3+} : Yb^{3+} :Er^{3+} = 80 : 18 : 2), 2.4 mmol of NaCl and 1.5 g of PAAs were dissolved in 20 mL ethylene glycol (EG) and mixed thoroughly to form a transparent solution. Then NH_4F (5 mmol) dissolved in 15 mL EG was added to the above mixture under stirring. The resulting mixture was transferred into a 50 mL Teflon-linked autoclave. The autoclave was then sealed and heated to 200 °C for 12 h. After cooling down to room temperature, the products were collected by centrifugation, washed with ethanol and distilled water several times, and dried in an oven at 60 °C.

2.3 Conjugation of UCNPs to monoclonal antibody 5G4-G4

The conjugation of UCNPs and monoclonal antibody 5G4-G4 were prepared by (EDC/sulfo-NHS)-mediated amidation reaction. Typically, 10 mg of EDC and 10 mg of sulfo-NHS were dissolved in 5 mL of 1× PBS buffer solution containing 50 mg of UCNPs. After approximately 15 min, 2 mL of 1× PBS buffer solution containing *n* (0.1–1.0) mg of monoclonal antibody 5G4-G4 was introduced. The reaction lasted for 4 h at 37 °C under gentle mixing. The products were collected by centrifugation, washed with PBS buffer three times. Then the resultant mixture was stored at 4 °C overnight.

2.4 Lateral flow immunochromatographic assay

The 4 mm-wide LFIA strip consists of five components including a sample pad for applying the sample solution, a conjugate pad for loading the particle-labeled antibody, a 25 mm long nitrocellulose membrane acting as the chromatography matrix, an absorbent pad serving as the liquid sink, and a backing card for supporting all the components (Fig. 1). Typically, at 5 mm from the absorbent pad, a band of goat anti-mouse IgG (1 mg mL^{-1}, Tiangen Biotech. Beijing, China) was manually drawn on the NC membrane as a control line (C line), while a band of 5G4-B8 (1 mg mL^{-1}) was drawn as the test line (T line) 10 mm from the conjugate pad.

Typically, the sample pad of 4 mm × 15 mm was pretreated by 1× PBS buffer containing 0.3% (w/v) PVP, and the conjugate pad of 4 mm × 5 mm was pretreated by PBS buffer containing 2% (w/v) BSA, 2% (w/v) Tween 20, and 2.5% (w/v) sucrose, 0.3% (w/v) PVP, respectively. Then, 25 μL solution of the as-prepared

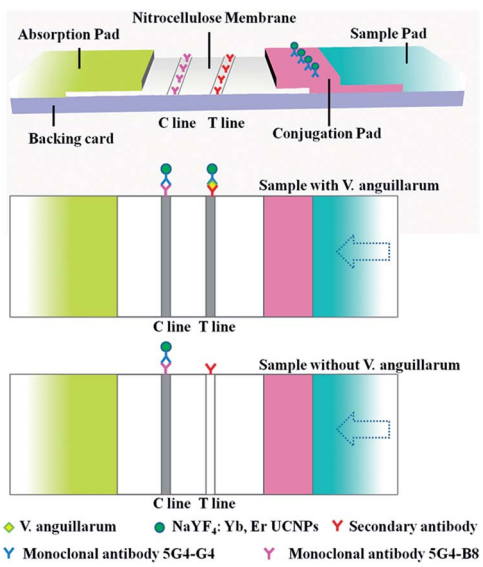

Fig. 1 The schematic image of the configuration and the principle of the detection.

particle-antibody conjugate was spotted on the conjugate pad. After the aforementioned LFIA components were dried properly, they were assembled with the overlaps between the sample pad and conjugate pad and that between the conjugate pad and the NC membrane being 5 mm to ensure the solution is migrating properly through the strip during the detection.

The following LFIA experiments upon competitive assay were run as follows. In brief, 100 μL solution of *V. anguillarum* MVM425 with a series of concentrations in 1× PBS buffer was applied to the sample pad. Then, the relative UC fluorescence intensity of both T line and C line was acquired 15 min later. A CW NIR laser at $\lambda = 980$ nm was used to excite the UCNPs on the strip. The laser was fixed at an angle of 30° relative to the LF strip surface.

To evaluate the specificity of the current detection method for *V. anguillarum* MVM425, four pathogenic Vibrio species, *V. alginolyticus*, *V. parahaemolyticus*, *V. harveyi*, *V. vulnificus* and *Edwardsiella tarda* EIB202, *Streptococcus iniae*, *Escherichia coli* CC118, *Staphylococcus aureus* were used for testing. The bacteria were grown to an exponential phase on a shaker at 30 °C in 250 mL flasks containing tryptic soy broth (TSB, Difco). TSB supplemented with 2% (w/v) NaCl was used for all *Vibrio* species. Bacterial pellets were washed twice with sterile phosphate buffered saline PBS and adjusted to 2.0×10^9 CFU mL^{-1}. The following LFIA experiments were carried out in the same way as mentioned above for *V. anguillarum* MVM425. Integrated fluorescent strips were stored in a self-sealing plastic bag with desiccant at 4 °C.

2.5 Characterization

To demonstrate the overall uniformity and morphology of the particles, the samples were characterized by scanning electron microscopy (SEM) using JEOL SM-6360LV microscope equipped with an energy dispersive X-ray spectroscopy (EDS). Transmission electron microscopy (TEM) images were taken with a JEOL 2011 microscope (Japan) operated at 200 kV. The crystal structure was investigated by X-ray power diffraction (RIGAK, D/MAX 2550 VB/PC, Japan). Fluorescence spectra were measured on a Fluorolog-3-P UV-VIS-NIR fluorescence spectrophotometer (Jobin Yvon, France), with a CW NIR laser at $\lambda = 980$ nm as the excitation source. The Fourier transform infrared (FTIR) spectra were recorded on a Nicolet5700 Fourier transform infrared spectrometer within the range of 500–4000 cm^{-1}.

3. Results and discussion

In the present work, $NaYF_4$: 18% Yb, 2% Er was synthesized by a solvothermal route in the presence of PAAs, since $NaYF_4$ has been reported to be the most efficient host material for Yb,Er co-doped NIR to visible upconversion phosphors.[30,31] PAAs is a multidentate capping reagent that can coordinate to the UCNPs surface through multiple $–COO^-$ groups, while an abundance of uncoordinated $–COO^-$ groups of PAAs will extend into the solution. The presence of free carboxyl groups on the surfaces not only results in high solubility of the UCNPs in aqueous solution, but also facilitates the conjugation of UCNPs with various biomolecules.[21]

The structures of the prepared $NaYF_4$:Yb,Er nanoparticles were characterized by powder X-ray diffraction (XRD) analysis, shown in Fig. 2. All the diffraction peaks can be indexed to a hexagonal phase of $NaYF_4$:Yb,Er (JCPDS 28-1192),[32] the absence of any other phase in the XRD indicates the high purity of the as-made sample. The sharp diffraction peaks indicate the high crystallinity under solvothermal conditions. The SEMs of $NaYF_4$:Yb,Er NPs are displayed in Fig. 3a and b, the as-synthesized samples consist of highly uniform spherical NPs, with an average diameter of 200 nm and a rough surface. The obvious lattice fringes in the HRTEM images (Fig. 3c) confirm the high crystallinity. The interplanar distances between adjacent lattice planes (0.30 nm) is well coincident with the (110) plane of $NaYF_4$:Yb,Er. The hexagonal phase structure of the UCNPs is further identified by the selected area electron diffraction (SAED) pattern (Fig. 3c, inset), which shows the spotty polycrystalline diffraction rings corresponding to the specific (100), (210) planes of the hexagonal $NaYF_4$:Yb,Er lattice. SEM examination of a selected area of $NaYF_4$:Yb,Er NPs combined with the corresponding EDS spectra (Fig. 3d) were taken at a number of selected positions of the sample and the elemental signatures of Na, Y, F, Er, and Yb are essentially identical within experimental accuracy.

The FTIR spectrum of PAAs modified $NaYF_4$:Yb,Er is shown in Fig. 4. The UCNPs exhibit a broad band at around 3440 cm^{-1}, corresponding to the O–H stretching vibration. The presence of –COOH in the functionalized UCNPs is confirmed by the bands in the region of 1400–1800 cm^{-1}, the band at 1422 cm^{-1} should be due to the C–O stretching vibration of the carboxyl groups and the two strong bands centered at 1567 cm^{-1} and 1457 cm^{-1} are associated with the asymmetric and symmetric stretching vibration modes of carboxylate anions, suggesting the effective $–COO–RE^{3+}$ complexation on the UCNPs surface. Meanwhile, the band at 1723 cm^{-1} is assigned to the C=O stretching vibration of the free carboxyl groups on the PAA polymer chain.[33]

The conjugation between monoclonal antibody and the UCNPs was realized by amidation reaction mediated by EDC and sulfo-NHS. The protein concentration was determined by

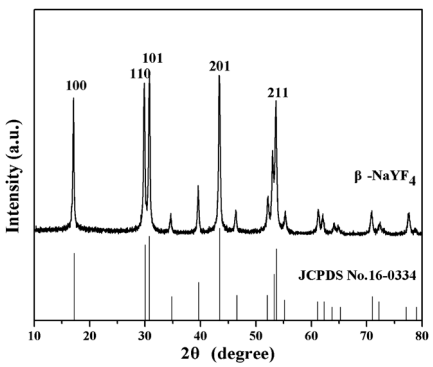

Fig. 2 The wide-angle XRD patterns of $NaYF_4$:Yb,Er UCNPs.

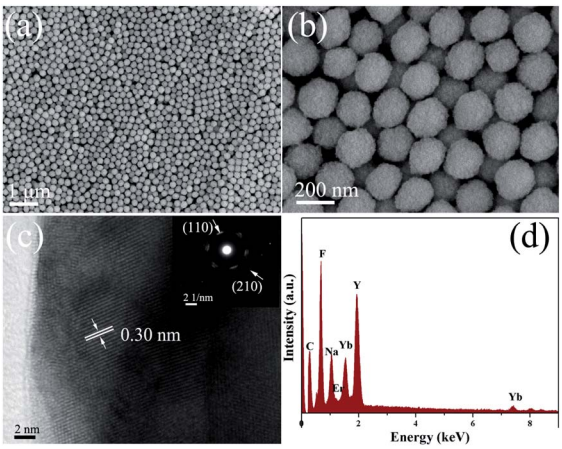

Fig. 3 (a) SEM image and (b) higher magnification SEM image of $NaYF_4$:Yb,Er NPs. (c) HETEM image of $NaYF_4$:Yb,Er NPs, insert displays the corresponding SEAD image. (d) EDS spectrum of the as-prepared $NaYF_4$:Yb,Er NPs.

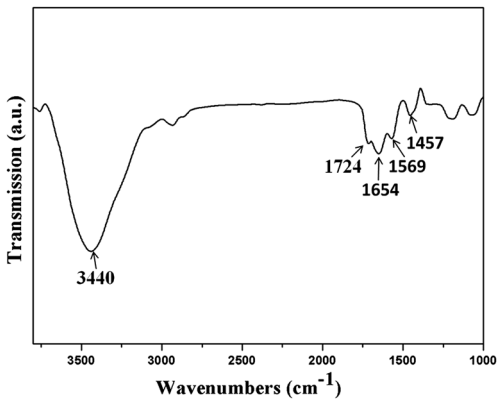

Fig. 4 FTIR spectrum of $NaYF_4$:Yb,Er NPs modified with PAAs.

the Bradford method using bovine serum albumin as a standard,[34,35] therefore residual antibody investigations were adopted to confirm the conjugation reaction between the UCNPs and antibody by determining the concentration variation of the antibody. The results in Fig. 5a show that the optimal amount of antibody is 0.4 mg, while the amount of UCNPs is 50 mg. Typical UC emission spectra of $NaYF_4$ NPs and UCNPs-antibody at the excitation of 980 nm are shown in Fig. 5b. The three peaks at 520 nm, 540 nm and 654 nm in the spectrum can be assigned to the $^2H_{11/2} \rightarrow {}^4I_{15/2}$, $^4S_{3/2} \rightarrow {}^4I_{15/2}$ and $^4F_{9/2} \rightarrow {}^4I_{15/2}$ transition, respectively.[36] The peak for the UCNPs-conjugates was very similar to that of the $NaYF_4$ NPs. The results suggest that the conjugation of antibody did not affect the UC fluorescence intensity of the $NaYF_4$ NPs.[37–39]

In the following LFIA experiments, the *V. anguillarum* MVM425 detection was performed by using the bioconjugates mentioned above. When an aqueous solution of target analyte *V. anguillarum* MVM425 was applied onto the sample pad, the UCNPs-antibody conjugates would have dissolved, and these substances would have migrated together to the absorbent pad

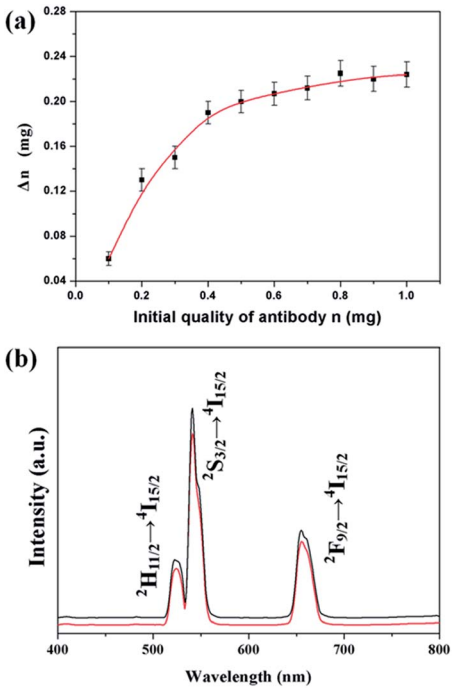

Fig. 5 (a) Binding capacity of antibody 5G4-G4 on UCNPs with different initial antibody quality. (b) UC emission spectrum of $NaYF_4$:Yb,Er UCNPs (black line) and UCNPs-antibody (red line).

by capillary force. The analyte *V. anguillarum* MVM425 could specifically bind with UCNPs-antibody conjugates on the conjugate pad if there was analyte in the sample solution. Then conjugates UCNPs-antibody-analyte could be captured by the monoclonal antibody 5G4-B8 immobilized on the T line. The excess fluorescent probes would have reacted with the goat anti-mouse antibodies and become trapped in the C line. After a complete assay, the fluorescent strip was subjected to fluorescence detection (Fig. 6a). Positive and negative results could be differentiated by observing whether or not fluorescent peaks appeared in the control and test lines. Both the UCNPs-antibody conjugates and the antibody immobilized on the T line can specifically bind with analyte *V. anguillarum* MVM425 at different binding sites, as shown in Fig. 1. The more analytes in the sample, the more fluorescently labeled conjugates would have bound to the capturing antibodies in the T line; this increase would have led to an increase in the fluorescence signal. Therefore, the fluorescence signal was proportional to the analyte concentrations in the sample; this fact could be used to quantify the *V. anguillarum* in the samples.[40] If no line was present in the fluorescent strip, or only one line was observed in the test line, the test was considered to be invalid.

In order to quantitatively extract the detection limit of the current LFIA method, the test strips were further subjected to UC fluorescence intensity analysis. The 10-fold serial dilution of *V. anguillarum* MVM425 suspension ranging from 10^9 to 10^1 CFU mL^{-1} in 1× PBS buffer solution were prepared and used in the following experiments. After loading 100 μL of analyte solution on the sample pad and running at room temperature for 15 min, we observed that the UC fluorescence intensity of

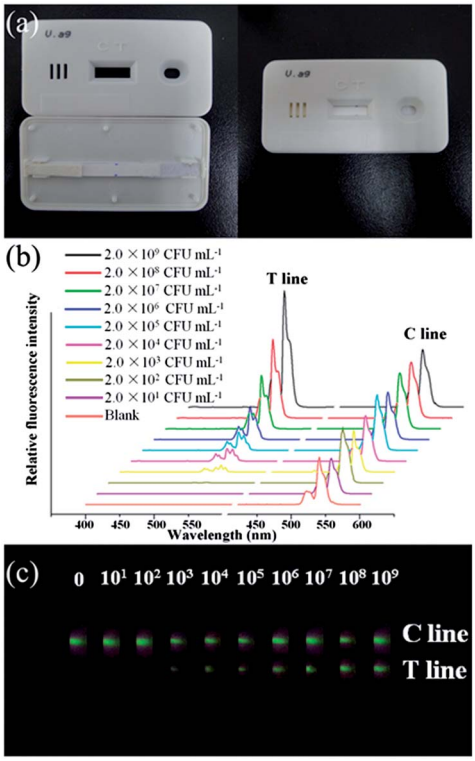

Fig. 6 (a) Photograph of the fluorescent strip in the cassette. (b) The emission spectra of T line and C line in relation to the added amount of *V. anguillarum* MVM425 under CW excitation at 980 nm. (c) Images of test strip (membrane area) taken using a 10-fold serially diluted *V. anguillarum* MVM425 solutions and a negative control in the assay buffer under excitation of a 980 nm CW diode laser.

the T lines was proportional to the concentration of *V. anguillarum* MVM425 (Fig. 6c). The typical UC fluorescence signals of T line from the strip reader increased with concentration increases of *V. anguillarum* MVM425 concentration, as shown in Fig. 6b. A blank control solution without analytes was applied for comparison. When there was no analytes in solution, there were no fluorescent signal on T line, which proved the results were valid. A distinct increase of UC fluorescence intensity in the spectrum was observed in the range of 10^3 to 10^9 CFU mL^{-1}, fluorescent signals were hardly to identified with smaller concentration. More exactly, as shown in Fig. 7, the linear was very good from 10^3 to 10^9 CFU mL^{-1} with a correlation coefficient $R^2 = 0.994$. The detection limit was calculated as the concentration that corresponded to three times the SD of the background signal, a value of 10^2 CFU mL^{-1} was determined.[41] The signals on both the T line and C line averaged from three parallel runs. This sensitivity is at least 100 times lower than ELISAs reported about *V. anguillarum*.[42–44]

Along with the sensitivity requirement, high specificity is crucial for the detection. The specificity of the immunoassay is normally associated with the antibody-antigen binding specificity. Therefore, to evaluate the specificity of the probe, eight commonly used pathogens were used under the same condition. Fig. 8 presents the UC fluorescence emission intensity of the T line of solutions containing the corresponding pathogens and a blank sample. Remarkably, it can be seen that only *V. anguillarum* MVM425 lead to bright UC fluorescence emission, which is attributed to the specifically binding of *V. anguillarum* MVM425 and monoclonal antibody 5G4-B8. This results show that it is sufficient for differentiation of *V. anguillarum* MVM425 from other Vibrio species. No cross-reaction with other pathogens was detected. Therefore, the UCNPs-antibody probe shows a high selectivity for *V. anguillarum* MVM425 against other pathogens.

To evaluate the stability of the UC fluorescent strips, the control sample (containing 10^3 CFU mL^{-1} *V. anguillarum* MVM425) can be used to evaluate the activity of the antibodies on the T line. If the antibodies and UC fluorescence conjugates have activity, then fluorescence would appear on the T line and C line. This test can be used to confirm that the UC fluorescent strips function well. Otherwise, the strip is out of function, and should be discarded. We investigated the strips *via* periodical testing using control samples, and found that the fluorescent strips could be maintained for up to 12 weeks if they were stored properly.

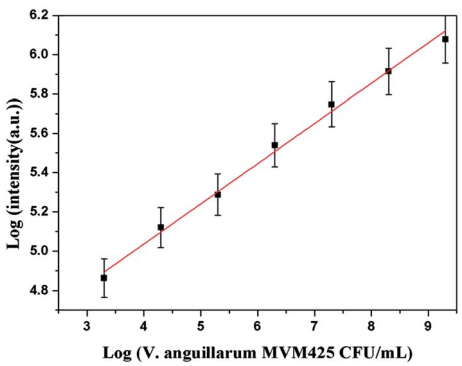

Fig. 7 Plot of the logarithm of relative fluorescence intensity *versus* the logarithm of the concentration of *V. anguillarum* MVM425.

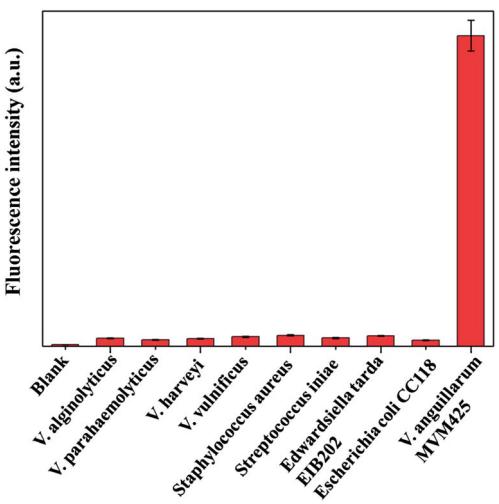

Fig. 8 The selectivity of UCNPs-antibody biosensor for different common pathogens.

4. Conclusion

In summary, a highly sensitive and specific UC fluorescence strip sensor is established *via* the use of UCNPs instead of colloidal gold commonly adopted in conventional LFIA. Carboxyl-modified β-$NaYF_4$: Yb,Er NPs were synthesized by a facile one-pot solvothermal approach, which were convenient to cross-link with monoclonal antibody. Because of the low autofluorescence, the UCNPs offer a greatly improved detection limit in detecting *V. anguillarum*, reaching 10^2 CFU mL^{-1}, in addition to excellent detection specificity and stability. Therefore, the current method would provide a highly sensitive detection method for hazardous pathogens in the future.

Acknowledgements

This work was supported by the National Natural Science Foundation of China (21236003, 21206042, 20925621, and 21176083), the Basic Research Program of Shanghai (13NM1400700, 13NM1400701), and the Fundamental Research Funds for the Central Universities.

References

1 J. Martinez-Picado, A. R. Blanch and J. Jofre, *Appl. Environ. Microbiol.*, 1994, **60**, 732.
2 H. I. Reid, J. W. Treasurer, B. Adam and T. H. Birkbeck, *Aquaculture*, 2009, **288**, 36.
3 M. Wang, J. Dai, S. Zhang, *et al.*, *Acta Oceanol. Sin.*, 2000, **22**, 132.
4 C. Cepeda, S. Garcia-Marquez and Y. Santos, *J. Fish Dis.*, 2003, **26**, 65.
5 A. Kulkarni, C. M. A. Caipang, M. F. Brinchmann, K. Korsnes and V. Kiron, *J. Rapid Methods Autom. Microbiol.*, 2009, **17**, 476.
6 N. L. Rosi and C. A. Mirkin, *Chem. Rev.*, 2005, **105**, 1547.
7 N. Bogdan, E. M. Rodriguez, F. Sanz-Rodriguez, M. C. I. de la Cruz, A. Juarranz, D. Jaque, J. G. Sole and J. A. Capobianco, *Nanoscale*, 2012, **4**, 3647.
8 C. D. Medley, J. E. Smith, Z. W. Tang, Y. R. Wu, S. Bamrungsap and W. H. Tan, *Anal. Chem.*, 2008, **80**, 1067.
9 X. Xu and C. A. Mirkin, *Angew. Chem., Int. Ed.*, 2007, **46**, 3468.
10 L. Wang, X. Liu, X. Hu and C. H. Fan, *Chem. Commun.*, 2006, **36**, 3780.
11 H. Wei, B. Li, J. Li and S. J. Dong, *Chem. Commun.*, 2007, **36**, 3735.
12 J. Wang, *Chem. Rev.*, 2008, **108**, 814.
13 J. Zhang, S. Song, L. Wang, D. Pan and C. H. Fan, *Nat. Protoc.*, 2007, **2**, 2888.
14 W. Chen, C. F. Peng, Q. H. Jin, C. L. Xu and W. Y. Wang, *Biosens. Bioelectron.*, 2009, **24**, 2051.
15 X. Y. Jiang, J. M. K. Ng, A. Stroock, S. K. W. Dertinger and G. M. Whitesides, *J. Am. Chem. Soc.*, 2003, **125**, 5294.
16 G. D. Liu, Y. Y. Lin, J. Wang, H. Wu, C. M. Wai and Y. H. Lin, *Anal. Chem.*, 2007, **79**, 7644.
17 H. L. Xie, W. Ma and L. Q. Liu, *Anal. Chim. Acta*, 2009, **634**, 129.
18 B. H. Liu, Z. J. Tsao, J. J. Wang and F. Y. Yu, *Anal. Chem.*, 2008, **80**, 7029.
19 P. Corstjens, M. Zuiderwijk, A. Brink, S. Li, H. Feindt, R. S. Niedbala and H. Tanke, *Clin. Chem.*, 2001, **47**, 1885.
20 P. Corstjens, M. Zuiderwijk, M. Nilsson, H. Feindt, R. S. Niedbala and H. Tanke, *Anal. Biochem.*, 2003, **312**, 191.
21 L. Huang, L. Zhou, Y. Zhang, C. Xie, J. Qu, A. Zeng, H. Huang, R. Yang and X. Wang, *IEEE Sens. J.*, 2009, **9**, 1185.
22 H. Na, K. Woo, K. Lim and H. S. Jang, *Nanoscale*, 2013, **5**, 4242.
23 Y. S. Liu, D. T. Tu, H. M. Zhu, R. F. Li, W. Q. Luo and X. Y. Chen, *Adv. Mater.*, 2010, **22**, 3266.
24 Y. Dai, H. Xiao, J. Liu, Q. Yuan, P. Ma, D. Yang, C. Li, Z. Cheng, Z. Hou, P. Yang and J. Lin, *J. Am. Chem. Soc.*, 2013, **135**, 18920.
25 P. Zhao, Y. Zhu, X. Yang, K. Fai, J. Shen and C. Li, *RSC Adv.*, 2012, **2**, 10592.
26 Y. Dai, P. Ma, Z. Cheng, X. Kang, X. Zhang, Z. Hou, C. Li, D. Yang, X. Zhai and J. Lin, *ACS Nano*, 2012, **6**, 3327.
27 C. Li and J. Lin, *J. Mater. Chem.*, 2010, **20**, 6831.
28 M. Haase and H. Schäfer, *Angew. Chem., Int. Ed.*, 2011, **50**, 5808.
29 J. Hampl, M. Hall, N. A. Mufti, Y. M. Yao, D. B. MacQueen, W. H. Wright and D. E. Cooper, *Anal. Biochem.*, 2001, **288**, 176.
30 J. C. Boyera and F. C. J. M. van Veggel, *Nanoscale*, 2010, **2**, 1417.
31 F. Wang and X. Liu, *Chem. Soc. Rev.*, 2009, **38**, 976.
32 P. Zhao, Y. Zhu, X. Yang, J. Shen, X. Jiang, J. Zong and C. Li, *Dalton Trans.*, 2014, **43**, 451.
33 K. W. Kramer, D. Biner, G. Frei, H. U. Gudel, M. P. Hehlen and S. R. Luthi, *Chem. Mater.*, 2004, **16**, 1244.
34 Y. Mao, T. Tran, X. Guo, J. Y. Huang, C. K. Shih, K. L. Wang and J. P. Chang, *Adv. Funct. Mater.*, 2009, **19**, 748.
35 H. P. Zhou, C. H. Xu, W. Sun and C. H. Yan, *Adv. Funct. Mater.*, 2009, **19**, 3892.
36 F. Wang, Y. Han, C. S. Lim, Y. Lu, J. Wang, J. Xu, H. Chen, C. Zhang, M. Hong and X. Liu, *Nature*, 2010, **463**, 1061.
37 S. Gai, P. Yang, C. Li, W. Wang, Y. Dai, N. Niu and J. Lin, *Adv. Funct. Mater.*, 2010, **20**, 1166.
38 Z. Wang, J. Hao, H. L. W. Chan, W. Wong and K. Wong, *Small*, 2012, **8**, 1863.
39 G. S. Yi and G. M. Chow, *Adv. Funct. Mater.*, 2006, **16**, 2324.
40 F. Zhang, M. Q. Zou, Y. Chen, J. F. Li, Y. F. Wang, X. H. Qi and Q. Xue, *Biosens. Bioelectron.*, 2014, **51**, 29.
41 J. H. Cho, E. H. Peak and I. H. Peak, *Anal. Chem.*, 2005, **77**, 4091.
42 S. F. Gonzale, C. R. Osorio and Y. J. Santos, *J. Fish Dis.*, 2004, **27**, 617.
43 J. L. Romalde, B. Magarinos, B. Fouz, I. Bandin, S. Nunez and A. E. Toranzo, *Dis. Aquat. Org.*, 1995, **21**, 25.
44 Z. Zhang, P. Zhang, Z. Mo, C. Wang and Y. Yu, *Acta Oceanol. Sin.*, 2005, **24**, 155.

